Activity of Peroxo and Hydroperoxo Complexes of Ti^{IV} in Olefin Epoxidation: A Density Functional Model Study of Energetics and Mechanism

Ilya V. Yudanov,[a,b] Philip Gisdakis,[a] Cristiana Di Valentin,[a,c] and Notker Rösch*[a]

Keywords: Density functional calculations / Epoxidation / Peroxo complexes / Titanium / Transition states

Epoxidation of olefins by Ti^{IV} peroxo and hydroperoxo (alkylperoxo) complexes was investigated using a hybrid DFT method (B3LYP). Reaction energies and activation barriers for direct oxygen transfer to ethylene as a model olefin were computed for various model complexes to compare the epoxidation activity of Ti(η^2-O_2) and TiOOR (R = H, CH_3) moieties. The activity of complexes with a Ti(O_2) peroxo group is shown to be essentially quenched when the coordination sphere of the complex is saturated by strongly basic (σ-donor) ligands. In contrast, the activity of a TiOOH functional group depends only weakly on the saturation of the coordination sphere of the Ti center. Substitution of methyl for hydrogen in a TiOOH group is found to slightly increase the activation barrier of epoxidation. The computational results give preference to reaction paths that involve TiOOR species. The factors governing the activity of Ti(O_2) and TiOOR groups, in particular the effects of donor ligands, are discussed on the basis of a molecular orbital analysis.

Introduction

Titanium(IV) peroxo species represent an active component in a number of homogeneous and heterogeneous oxidation reactions of organic substrates by hydrogen or alkyl peroxides.[1] Important examples of catalytic processes of this type are the homogeneous stereoselective epoxidation of allylic alcohols by alkyl peroxides catalyzed by Ti^{IV} alkoxides (Sharpless epoxidation)[2] and the heterogeneous epoxidation of olefins on titanium silicates (or silicalites) with amorphous[3] or zeolite-like structures.[4] Despite intense experimental work, the precise structure of the oxidizing active site is still a matter of controversy in most of cases, especially for heterogeneous catalytic processes on titanium silicates.[4–6]

In the known epoxidation reactions, titanium hydroperoxo or alkylperoxo groups, TiOOR (R = H, alkyl), are generally accepted as oxygen donors, while peroxo groups, Ti(η^2-O_2), with two symmetrically coordinated oxygen centers at Ti are considered inert in this reaction. For instance, a TiOO-*t*Bu species is assumed to be responsible for epoxidation in the Sharpless process,[7] and a TiOOH species for epoxidation on Ti silicalite.[4] In early reports active Ti(O_2) species have also been suggested for the latter system.[8][9] Actually, a number of stable and experimentally well-characterized Ti^{IV} η^2-peroxo complexes are not active in olefin epoxidation, e.g. (TPP)Ti(O_2)[10] (TPP = tetraphenylporphyrin) and Ti(O_2)(pic)$_2$·HMPA[11] (HMPA = hexamethylphosphoric triamide; pic = picolinato). However, there is evidence[10] that (TPP)Ti(O_2) becomes active in the epoxidation of cyclohexene once it is transformed to the *cis*-hydroxo(alkylperoxo) complex (TPP)Ti(OH)(OOR), although the latter has never been isolated.

On the other hand, the η^2-peroxo or bis-peroxo d^0 complexes of Mo, W, and Re, which are structurally similar to Ti(O_2) species, are known to epoxidize alkenes.[1,12,13] Thus far, no clear rationalization has been presented as to why η^2-peroxo complexes of Ti are not active in epoxidation. The inactivity of (TPP)Ti(O_2) has been rationalized by steric repulsion between the alkene and the porphyrin ring.[1] However, electronic effects of the porphyrin ring on the properties of the peroxo group might provide a different reason, by analogy with the inhibiting effect of strong coordinating solvents on the epoxidation activity of the bis-peroxo molybdenum complex $MoO(O_2)_2 \cdot HMPA$.[14] Here, the reactivity decrease of the peroxo group under coordination of a seventh ligand to the metal center has been attributed[15][16] to electronic effects rather than to the possibility that the reacting alkene may be prevented from coordinating to the Mo center. An inhibiting electronic effect of basic ligands on the activity of Re and Mo bis-peroxo complexes has also recently been demonstrated computationally.[17–19]

Several theoretical investigations on ethylene epoxidation catalyzed by Ti^{IV} species have been reported.[20–24] These studies presented structures of possible intermediates as well as activation energies for oxygen transfer. Most of them dealt with models of hydroperoxo complexes like $(HO)_3$-TiOOH[20–22] or closely related clusters that partially account for a silicate surrounding, e.g. $(H_3SiO)_2(HO)$-TiOOH[24] and $(H_3SiO)_3(CH_3OH)$TiOOH.[23] The activity

[a] Institut für Physikalische und Theoretische Chemie, Technische Universität München,
D-85747 Garching, Germany
Fax: (internat.) +49 (0)89/289 13622
E-mail: roesch@ch.tum.de
[b] Permanent address: Boreskov Institute of Catalysis, Siberian Branch of Russian Academy of Sciences,
630090 Novosibirsk, Russia
[c] Permanent address: Dipartimento di Chimica Organica, Università degli Studi di Pavia,
V. le Taramelli 10, I-27100 Pavia, Italy

  1434–1948/99/1212–2135 $ 17.50+.50/0

of $Ti(O_2)$ species was investigated only with the model peroxo complex $(HO)_2(H_2O)Ti(O_2)$.[22] Note that the Ti center of most models studied is five-coordinated. This is lower than the typical coordination (six or seven) of the experimentally characterized Ti^{IV} peroxo and alkylperoxo complexes,[11,25–27] i.e. the coordination sphere of these Ti model complexes is not saturated. Under reaction conditions the coordination of Ti centers in titanium silicalites expands beyond the initial tetrahedral structure.[28] Despite there being a number of particular cases that have been considered, a comprehensive computational comparison of properties of $Ti(O_2)$ and TiOOR species and their epoxidation activity is still lacking.

With the present work on Ti^{IV} complexes we continue our series of density functional (DF) investigations on olefin epoxidation in which we have so far studied Re, Cr, Mo, and W d^0 peroxo complexes.[17–19] Here, we compare the epoxidation activity of a number of Ti^{IV} model complexes that contain either peroxo or hydroperoxo (alkylperoxo) functional groups. For this purpose we have calculated the reaction energies and the activation barriers for direct oxygen transfer from both types of peroxo groups, $Ti(\eta^2\text{-}O_2)$ and TiOOR, to the model olefin ethylene. In addition, we pay special attention to the coordination number of the Ti center. The model study presented here will also shed light on the mechanism of epoxidation on titanium silicates.

The goals of the present study are (i) to investigate the mechanism of olefin (ethylene) epoxidation by Ti complexes with peroxo and hydroperoxo (alkylperoxo) functional groups; (ii) to determine factors that govern the reactivity of these groups and, in particular, to study the dependence of the activity on the saturation of the coordination sphere of central Ti ion; and (iii) to consider the effect of an alkyl substituent of the TiOOR moiety on the activation barrier of epoxidation.

Results and Discussion

We intend to focus on the electronic effects of ligands on the properties of the moieties $Ti(O_2)$ and TiOOR, but we want to leave aside steric effects. Therefore, we start with simple monodentate ligands like hydroxyl groups as anionic ligands and ammonia or water as (neutral) σ donors. In this way, we are able to relate the models under study to different types of titanium peroxo compounds: either to complexes with more complicated polydentate organic ligands or to Ti species incorporated in silicate structures. In order to make this relation more realistic we consider at the end models where some hydroxide ligands are replaced by either methoxide or siloxide ligands. We shall take solvent effects into account only through the coordination of additional ligands to the Ti center; no other environment effects are included. However, from studies on Re and Mo peroxo complexes it is known[17][29] that long-range solvent effects and zero-point energy corrections hardly influence reaction energies and activation barriers of oxygen transfer to olefins.

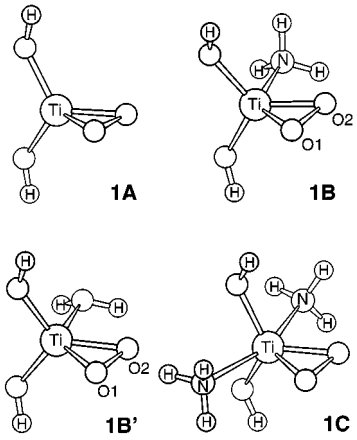

Figure 1. Model complexes with a $Ti(\eta^2\text{-}O_2)$ functional group

Model Complexes

We start by considering model η^2-peroxo complexes of Ti^{IV}. The simplest such model is $(HO)_2Ti(O_2)$, **1A** (Figure 1), with the peroxo group coordinated to Ti in a symmetric η^2 ("side-on") fashion; two hydroxyl ligands provide the oxidation state IV and electro-neutrality of the complex. The coordination sphere of complex **1A** is far from saturated and thus **1A** exhibits significant affinity to basic ligands. The binding energy of further ligands is −32.3 kcal/mol for NH_3 (complex **1B**, Figure 1) and −25.9 for H_2O (**1B′**). Addition of a second NH_3 molecule to **1B** leads to a further energy gain of −16.5 kcal/mol. The resulting complex, **1C** (Figure 1), can be considered as a model of the complex $Ti(TPP)(O_2)$ with the porphyrin ring of the latter substituted by two NH_3 and two hydroxide ligands. Geometry optimizations of the complexes **1A** and **1C** converged to structures with effective C_{2v} symmetry; thus in these complexes the two oxygen centers of the peroxo group are essentially equivalent. In complexes with one basic ligand, **1B** and **1B′**, the symmetry of the peroxo group is slightly distorted with the Ti−O distances differing by 0.02 Å (see Table 1). The calculated structural parameters of the titanium peroxo group (Table 1) are in very good agreement with X-ray data of known Ti^{IV} peroxo complexes.[11,25,26] For instance, the calculated Ti−O and O−O distances of 1.86 and 1.46 Å, respectively, in the peroxo group of complex **1C** are very close to the corresponding experimental values of 1.83 and 1.45 Å, respectively, of the complex $(OEP)Ti(O_2)$ (OEP = octaethylporphyrinato),[26] where Ti also exhibits coordination number 6.

Models of Ti hydroperoxo (alkylperoxo) complexes are shown in Figure 2. Complex **2A** has previously been used for modeling active intermediates of the Sharpless epoxidation[20] and epoxidation centers of Ti-silicalites.[21][22] Model **2B** is derived from **2A** by adding an NH_3 ligand; the calculated ligand binding energy is −13.2 kcal/mol. Model **3A** differs from **2A** by a methyl substituent in place of the hydrogen center of the peroxo group. The fact that no local symmetry in the Ti(OOR) moiety is preserved does not come as a surprise (Table 2). However, the hydroperoxo (alkylperoxo) ligand is still coordinated to Ti by both oxy-

Table 1. Calculated properties of Ti peroxo complexes: intermediates and oxygen transfer transition states. For the designation of the various structures see Figure 1

	1A	**1B**		**1B′**	**1C**
Geometry of peroxo group, Å					
r(O−O)	1.487	1.472		1.472	1.460
r(Ti−O1)	1.823	1.837		1.836	1.861
r(Ti−O2)	1.823	1.859		1.857	1.861
NBO atomic charges, e					
q(O1 front)	−0.45	−0.45		−0.44	−0.48
q(O2 back)	−0.45	−0.49		−0.50	−0.48
total *q*(OO)	−0.90	−0.94		−0.94	−0.96
q(Ti)	1.89	1.72		1.75	1.60
Core level energies, eV					
1s(O1)	−522.0	−520.9		−521.1	−520.2
1s(O2)	−522.0	−520.8		−521.0	−520.2
3s(Ti)[a]	−67.1	−66.0		−66.3	−65.3
Geometry of transition state, Å		front	back	front	
r(O−O)	1.856	1.863	1.854	1.860	1.847
r(Ti−O1)	1.875	1.929	1.731	1.913	2.001
r(Ti−O2)	1.741	1.748	1.965	1.752	1.739
r(O−C1)	2.211	2.110	2.064	2.108	2.020
r(O−C2)	2.211	2.109	2.070	2.141	2.027
Activation barrier, kcal/mol	11.0	19.0	22.3	17.4	27.4

[a] The 1s and 2s eigenvalues of Ti are not available because of the ECP description.

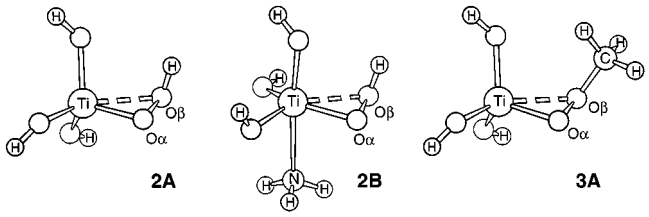

Figure 2. Model complexes with a TiOOR functional group (R = H, CH_3)

gen centers with Ti−Oα and Ti−Oβ distances (Figure 2) of about 1.89 and 2.27 Å, respectively. The plane OOR of the TiOOR group is almost orthogonal to the plane TiOO. The O−O distance is about 1.47 Å. The calculated structure of the TiOOR group agrees very well with recently reported data for {[(η^2-*tert*-butylperoxo)titanatrane]$_2$ · 3 dichloromethane}: *r*(Ti−Oα) = 1.913 Å, *r*(Ti−Oβ) = 2.267 Å, and *r*(O−O) = 1.469 Å.[27] This is the only alkylperoxo complex of Ti reported to date for which an X-ray crystal structure is available. Although the authors[27] chose to designate this structure as η^2, we will not use this notation for TiOOR complexes in the following discussion in order to distinguish them from Ti(O_2) complexes that do exhibit almost ideal η^2 coordination. Models **1B′** and **2A** have the same stoichiometry; a formal proton transfer from the water ligand of **1B′** to the peroxo group leads to **2A**. This transfer is calculated to be exothermic by −7.0 kcal/mol; thus, the hydroperoxo complex **2A** is more stable.

Epoxidation Transition States

In the study of the epoxidation activity of the various intermediates described above we calculated in each case the transition states of oxygen transfer to the model olefin ethylene. The corresponding species will be referred to by a prefix **TS**, e.g. **TS-1A** designates the transition state of ethylene epoxidation by complex **1A**. We focus on the oxygen transfer mechanism where the ethylene double bond directly attacks an oxygen center of the peroxo (hydroperoxo) group. The activation barriers are calculated with respect to the corresponding "free" complexes and an ethylene molecule. We shall neglect the physical interaction between ethylene and a peroxo group of the reaction intermediate in the ground state; this interaction is about 2 kcal/mol.[21]

In the following text we will not discuss the insertion mechanism of Mimoun, which implies that an olefin substrate first binds to the metal center and then inserts into the peroxo-metal bond in a [2 + 2] fashion to form a metallocycle intermediate.[12][14] For **1B** this metallocycle intermediate is calculated to lie 9.7 kcal/mol higher than the reactants and the corresponding activation barrier is 27.3 kcal/mol, while a direct attack requires only 19.0 kcal/mol for activation (Table 1). These findings are very similar to those for d^0 peroxo complexes of Re[17] and Mo[19] where, at the same level of computation, [2 + 2] insertion was shown to exhibit significantly higher activation barriers than a direct transfer.

The calculated transition states of the Ti(O_2) and TiOOR (R = H, CH_3) moieties have a number of features in common and, in general, resemble the structures of transition states of direct oxygen transfer for Re, Mo, and W.[17][19] All transition structures exhibit a spiro orientation of the ethylene unit (Figures 3 and 4), i.e. the plane CCO is almost orthogonal to the plane TiOO. The structure of the ethylene moiety is only slightly distorted from the gas phase structure: the C−C bond in the transition state is elongated by 0.04 Å at most. All these transition states represent a synchronous approach of ethylene to the peroxo moiety with almost equal distances between the carbon atoms and the attacked oxygen center. The largest difference between

Table 2. Calculated properties of Ti hydroperoxo (alkylperoxo) complexes: intermediates and oxygen transfer transition states. Structures **2A**, **2B**, and **3A** are shown in Figure 2. The models **4A/4B** and **5A/5B** are obtained after replacing equatorial OH groups in the models **2A/2B** by OCH_3 (Figure 9) and $OSiH_3$ groups, respectively

	2A	**2B**	**3A**	**4A**	**4B**	**5A**	**5B**
Geometry of peroxo group, Å							
r(O−O)	1.468	1.469	1.466	1.470	1.470	1.468	1.469
r(Ti−Oα)	1.891	1.918	1.888	1.899	1.926	1.892	1.923
r(Ti−Oβ)	2.262	2.276	2.265	2.256	2.268	2.237	2.243
NBO atomic charges, e							
q(Oα)	−0.46	−0.46	−0.46	−0.47	−0.47	−0.45	−0.45
q(Oβ)	−0.46	−0.47	−0.47	−0.46	−0.48	−0.45	−0.47
Total q(OO)	−0.92	−0.93	−0.93	−0.93	−0.95	−0.90	−0.92
q(Ti)	1.77	1.65	1.78	1.80	1.72	1.81	1.69
Core level energies, eV							
1s(Oα)	−521.8	−521.1	−521.6	−521.5	−520.9	−521.9	−521.3
1s(Oβ)	−522.8	−522.4	−522.7	−522.5	−522.2	−522.9	−522.6
3s(Ti)[a]	−66.7	−66.2	−66.6	−66.4	−65.9	−67.0	−66.6
Geometry of transition state, Å							
r(O−O)	1.790	1.768	1.820	1.794	1.802	1.800	1.783
r(Ti−O1)	1.954	2.013	1.957	1.966	2.001	1.969	1.998
r(Ti−O2)	2.061	2.064	2.032	2.059	2.095	2.042	2.067
r(O−C1)	2.202	2.165	2.170	2.187	2.079	2.170	2.117
r(O−C2)	2.120	2.160	2.071	2.111	2.187	2.111	2.186
Activation barrier, kcal/mol	12.7	12.4	15.8	14.5	13.6	15.0	13.7

[a] The 1s and 2s eigenvalues of Ti are not available because of the ECP description.

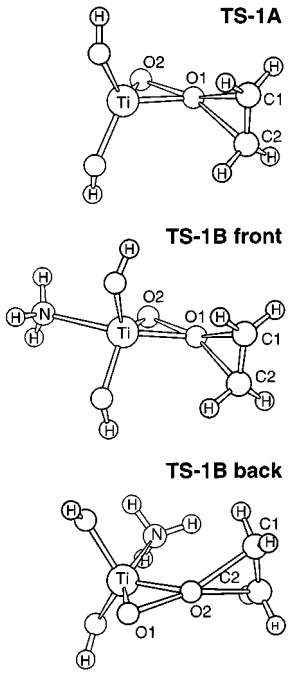

Figure 3. Transition states for direct oxygen transfer from various Ti peroxo complexes to an ethylene molecule

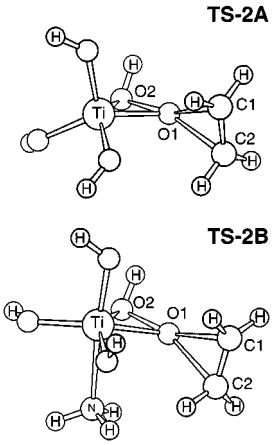

Figure 4. Transition states for direct oxygen transfer from the Ti hydroperoxo intermediates **2A** and **2B** to an ethylene molecule (α attack)

the O−C distances, about 0.03 Å, is found for **TS-1B′** (Table 1). The O−C distances of hydroperoxo complexes differ to a somewhat greater extent, at most by about 0.1 Å in **TS-3A** (Table 2). Similar synchronous transition states were calculated at the same level of computation (B3LYP) for the epoxidation of 1-pentene[30] and allyl alcohol[31] by peroxyformic acid. In the transition states of $Ti(O_2)$ intermediates, one of the Ti−O distances has increased by 0.05−0.14 Å whereas the other Ti−O distance has decreased by about 0.08 Å compared to the corresponding intermediates (Table 1). In the transition states of the TiOOR intermediates, the distance Ti−Oα has increased by 0.07−0.09 Å while the distance Ti−Oβ has decreased by about 0.16−0.21 Å (Table 2). The distances between the metal center and the attacked oxygen in peroxo and hydroperoxo transition states (Ti−O1 and Ti−Oα, respectively) are quite comparable and have values of about 1.9−2.0 Å (Tables 1 and 2). The most dramatic changes on the way to the transition state occur in the structure of the peroxo moiety: the O−O distance increases from about 1.47 Å in the intermediates to 1.82−1.86 Å in the peroxo transition states (Table 1) and to 1.89−1.92 Å in the hydroperoxo transition states (Table 2). A full vibrational analysis was performed for the transition state structures **TS-1B** (Figure 3) and **TS-2A** (Figure 4) as representatives of the two types of intermediates, $Ti(O_2)$ and TiOOR. Each of these structures was found to exhibit a single imaginary frequency; this confirms

the nature of the transition states as first-order saddle points on the corresponding potential energy hypersurfaces.

Oxygen transfer by epoxidation reaction involving d^0 metal peroxo complexes is generally accepted to exhibit electrophilic character.[1][12] This view is based on the fact that peroxo and alkylperoxo complexes react faster with electron-rich alkenes, e.g. with highly alkyl-substituted species. In a recent experimental study with peroxo compounds of V, Mo, and W the electrophilic nature of peroxo oxygen centers was also probed by sulfoxidation of thianthrene 5-oxide, in which an oxygen center of a peroxo complex attacks the electron-rich sulfide group rather than the electron-poor sulfoxide group.[32] In the present calculations, the electrophilic character of the oxygen transfer is manifested through the electron density transfer in the transition state, about 0.2 e, from ethylene to the peroxo (hydroperoxo) complex.

For $Ti(O_2)$ complexes the calculated activation barriers increase strongly in the sequence **1A**, **1B**, **1C**, from 11.0 to 27.4 kcal/mol (Table 1). The first complex of this family, **1A**, exhibits the lowest activation barrier, 11.0 kcal/mol, of all species considered in present work. An additional basic ligand significantly decreases the activity of the peroxo group, as deduced from the activation barriers of the complexes **1B** and **1B′**, which are 19.0 and 17.4 kcal/mol, respectively. It was found that the stronger the basic character of the ligand (ammonia vs. water), the higher the barrier. Note that in the models **1B** and **1B′** the oxygen centers of the peroxide group are not equivalent and, therefore, attacks of both centers have to be considered. We refer to attacks of the oxygen centers O1/O2, i.e. distant from/close to the NH_3 ligand (Figure 3), as "front" or "back" transition states.[17] In Table 1 we report the pertinent parameters of both transition states starting from complex **1B**. The back transition state corresponds to an attack of the more negative center O2, with the olefin in spatial proximity to the base. This situation leads to a somewhat higher barrier of 22.3 kcal/mol, which is in line with previous findings for Re, Mo, and W complexes.[17][19] The highest activation barrier of the peroxo series, 27.4 kcal/mol, is calculated for **1C** with two NH_3 ligands. Thus, saturation of the coordination sphere of the Ti center completely quenches the epoxidation activity of titanium peroxo group.

Analogous trends of increased activation energies concomitant with an increased number of basic ligands have been obtained in calculations on Re, Cr, Mo, and W mono- and bis-peroxo complexes.[17][19] A joint experimental and theoretical study[18] on different base adducts of the bis-peroxo complex $(O_2)_2(H_3C)Re{=}O$ revealed that coordination of a base to the complex induces, mediated by the metal center, additional electron density on the peroxo group; this pushes the *anti*-bonding $\sigma^*(O-O)$ level upward and results in a higher activation barrier (see below). Coordinatively saturated complexes of Re, Mo and W still exhibit moderate activation barriers ranging from 16 to 20 kcal/mol;[17–19] only Cr, which like Ti is a first row transition element, exhibits very high barriers for ethylene epoxidation. For example a barrier of about 40 kcal/mol is calculated for the model complex $(O_2)Cr(=O)_2 \cdot (NH_3)_2$,[19] which is structurally similar to our model **1C** but features oxo instead of hydroxide ligands. Experimental studies on the epoxidation activity of the bis-peroxo molybdenum complex $MoO(O_2)_2 \cdot HMPA$ have also rationalized the inhibiting effect of strongly coordinating solvents as an electronic effect of the additional (seventh) ligand on the properties of the peroxo group.[15][16] However, seven-coordinated $(L\text{-}L)MoO(O_2)_2$ complexes with bidentate L-L basic ligands were recently shown to catalyze epoxidation with *tert*-butyl hydroperoxide as an oxidant, and the formation of an MoOO*t*Bu group as an active center was proposed.[33]

For the TiOOR complexes we consider the α-attack to a peroxo group, i.e. transfer of the oxygen atom that is (closely) bound to the Ti center (Oα in Figure 2). β-attack, i.e. attack of the other oxygen center (with a substituent attached; Oβ in Figure 2), results in a higher activation energy; during this process the O−O bond breaks, accompanied by a proton transfer from Oβ to Oα. For instance, the activation barrier of ethylene epoxidation by **2A** via β-attack is calculated to be 25.7 kcal/mol, compared to 12.7 kcal/mol for α-attack. Similar differences in the barrier heights between α- and β-attack have also been found for hydroperoxo derivatives of Re and Mo.[17][19] At variance with the $Ti(O_2)$ complexes, the reaction barrier of TiOOR intermediates hardly changes upon addition of a donor ligand. Both transition states **TS-2A** and **TS-2B** feature relatively low activation energies of 12.7 and 12.4 kcal/mol, respectively. Thus, despite the additional NH_3 ligand, the activation barrier of **2B** is calculated to be slightly lower than the barrier of **2A**. This small decrease of the barrier height, by 0.3 kcal/mol, is in line with the change of the O−O distance (Table 2), although such minor changes are at the edge of computational accuracy.

Comparison to Other Computational Studies

Next, we shall comment on the absolute values of the calculated activation barriers and on the accuracy of our results. From MP2 calculations,[22] activation barriers have been reported for the front attack of **1B′**, 13.2 kcal/mol, and for the α-attack of **2A**, 14.4 kcal/mol, which are similar to the corresponding values of the present study, 17.4 and 12.7 kcal/mol, respectively. However, these MP2 values have been obtained under C_s symmetry constraints.[22] Two rather different values of the activation barrier of **2A**, 9 (with C_s symmetry constraints)[20] and 21[21] kcal/mol, have been determined in DF calculations where the gradient-corrected BLYP exchange-correlation functional was employed. Significant differences of structural parameters are also worth noting. The C_s symmetry constraints enforce a planar structure of the TiOOH moiety (Figure 2) with a significantly elongated Ti−Oβ distance, 2.6−2.7 Å[20–22] (compared to about 2.27 Å calculated in the present study; Table 1). On the other hand, when used without symmetry constraints the BLYP approach yields too short a value for

Ti−Oβ, 2.1 Å.[21] To check the effect of a C_s symmetry restriction for the present B3LYP investigations, we also calculated **1B′** and **2A** as well as the corresponding transition states **TS-1B′** (front) and **TS-2A** in this way; the resulting activation barriers are 16.1 and 13.8 kcal/mol, respectively. The differences from the corresponding values of full geometry optimizations are only about 1 kcal/mol, but are of opposite sign; thus, the selectivity between the two transition state structures is reduced.

To check for possible basis set effects and to justify the use of ECPs we also performed calculations with an all-electron TZV(f) basis for Ti. Single-point calculations with the geometry optimized in the standard approach (see Computational Details) yield activation barriers of 17.9 and 13.8 kcal/mol for **TS-1B′** (front) and **TS-2A**, respectively. Further optimization of the intermediate **1B′** and the transition state **TS-1B′** (front) leads to a uniform lowering of the total energy values by 0.5 kcal/mol for both structures with almost no effect on the height of the barrier; for **2A** the barrier changes by 0.1 kcal/mol only. These results show that the computational strategy used in the present study is quite accurate. As a further supporting argument, one notes that the structure of the TiOOH group calculated here is in very good agreement with available experimental data,[27] at variance with some earlier quantum chemical investigations.[20−22] The absolute accuracy of the B3LYP approach for activation barriers is another question altogether. However, a critical comparison shows that, at least for barrier heights of organic reactions, B3LYP performs significantly better than BLYP or MP2.[34][35]

Reaction Energies

For both types of species, $Ti(O_2)$ and TiOOR, ethylene epoxidation is an exothermic reaction. By this reaction, $Ti(O_2)$ species transform into complexes with a titanyl Ti=O functional group, while TiOOH species form a TiOH group after loss of one oxygen unit. The reaction energies are computed with respect to isolated products, namely the metal complex and ethylene oxide. The calculated reaction energies for $Ti(O_2)$ species increase from −23.8 kcal/mol for **1A** to −30.7, −31.2, and −34.1 kcal/mol for **1B′**, **1B**, and **1C**, respectively. Obviously, the higher reaction energy for highly coordinated species is due to higher stabilization of Ti=O product by basic ligands compared to initial $Ti(O_2)$ intermediate, since the coordination number of Ti is lower in the product complex due to the loss of one oxygen center. The complexes **2A** and **2B** exhibit significantly higher epoxidation reaction energies of −43.2 and −44.8 kcal/mol, respectively. The reaction profiles of the various $Ti(O_2)$ and TiOOH intermediates are represented in Figure 5 where the energy of the lowest intermediate **1C** + C_2H_4 is taken as reference. Inspection of Figure 5 reveals that the intermediates **1C** and **2B** feature the lowest energies and similar thermodynamic stability. However, epoxidation by **2B** is favored for both thermodymamic (higher reaction energy) and kinetic reasons (lower activation barrier). Evidently, the kinetic argument plays the key role here: epoxidation by the $Ti(O_2)$ intermediate **1C** can be ruled out since the corresponding transition state exhibits an activation barrier of more than 27 kcal/mol; this is more than twice as high as the activation barrier for the TiOOH intermediate **2B**.

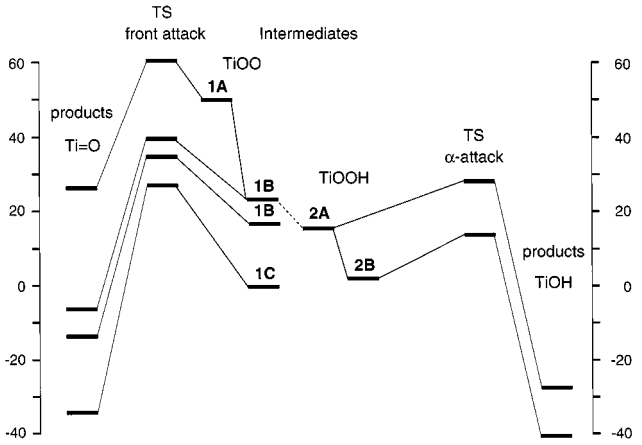

Figure 5. Total energies of intermediates with $Ti(O_2)$ or TiOOR groups and the corresponding transition states and products of ethylene epoxidation, relative to the energy of **1C** + C_2H_4. The activation barrier of proton transfer (dashed line) between the isomers **1B′** and **2A** is not shown

Molecular Orbital Analysis and Discussion

We turn to an analysis of the electronic structure of both types of the reaction intermediates, $Ti(O_2)$ and TiOOH, to rationalize the calculated activity trends. For this purpose, we consider a $Ti(O_2)$ moiety formally as an O_2^{2-} ligand coordinated to a Ti^{4+} d^0 center. The interaction between ligand and metal center can be considered as a donation from the peroxo group to the vacant d orbitals of Ti.

The energy of the unoccupied *anti*-bonding σ*(O−O) level is one of the most important of the factors that determine the activity of peroxo complex in oxygen transfer.[18] The activation of the O−O bond in the transition state is due to the interaction of this orbital in the LUMO group of the metal moiety with the HOMO π(C−C) of ethylene. The σ*(O−O) level is not the true LUMO of the complex; it lies slightly above the manifold of vacant d-levels of the metal center. The energy position of the σ*(O−O) level is expected to reflect the ability of peroxo group to accept additional electron density, which leads to breaking of O−O bond. This is indeed the case: the lower the energy of the σ*(O−O) level, the smaller is the calculated barrier for oxygen transfer. This is demonstrated in Figure 6a where the dependence of the activation barrier on the σ*(O−O) − π(C−C) gap is shown.

Coordination of a basic (σ-donor) ligand to **1A**, e.g. NH_3 in **1B**, increases the electron density at the peroxo group: the charge of the peroxo group given by a natural bond orbital analysis (NBO)[36] changes from −0.90 e in **1A** to −0.94 e in **1B** (and to −0.96 e in **1C** with two NH_3 ligands, Table 1). Concomitantly, the 1s(O) core level energies are shifted upward in **1B** by about 1.1 eV compared to **1A** (by

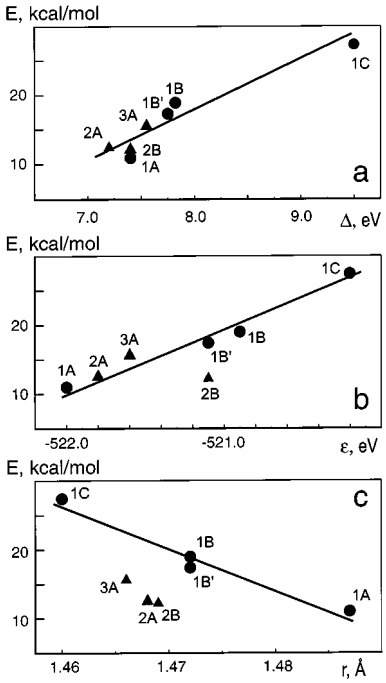

Figure 6. Calculated activation energy $\Delta E^{\#}$ (in kcal/mol) as function of (a) the HOMO−LUMO energy gap $\Delta = \sigma^*(O-O) - \pi(C-C)$ (in eV); (b) the energy ε (in eV) of the 1s(O) core level as a measure of negative charge located on the attacked oxygen center; (c) the O−O bond length (in Å). Data of peroxo group of $Ti(O_2)$ (circles) and TiOOR (triangles) complexes. Lines of linear regression on the data of the $Ti(O_2)$ complexes are also shown

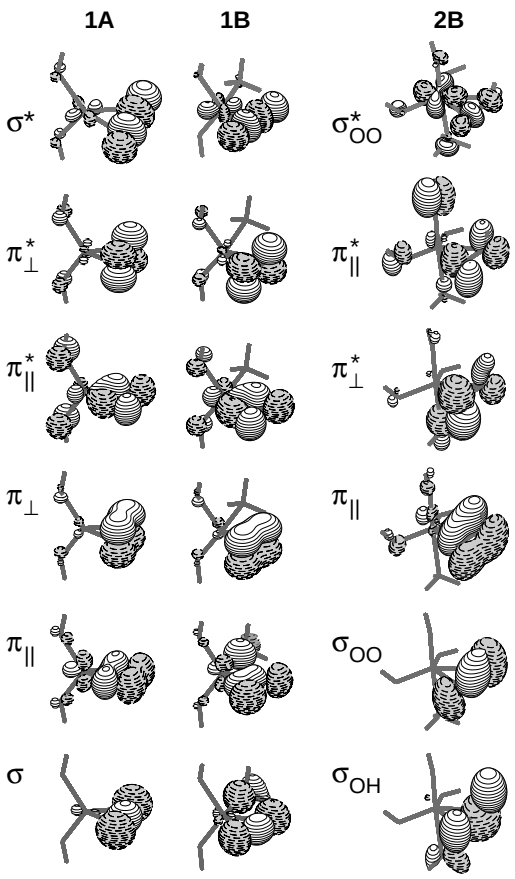

Figure 7. Structure of molecular orbitals of the intermediates **1A** (left), **1B** (center), and **2B** (right) with dominant contributions of the peroxo or hydroperoxo group

about 2.0 eV in **1C**); this is also indicative for an increase of electron density on the peroxo ligand. Thus, additional basic ligands reduce the donation from the peroxo ligand to the metal center; the electrophilic character that controls olefin epoxidation is also reduced.[1][12] Figure 6b shows how the 1s(O) core level energy as an indicator for the electron charge density of the peroxo or hydroperoxo moiety correlates with the calculated barrier of oxygen transfer.

Another factor determining the activation barrier of oxygen transfer is the strength of the O−O bond in the absence of an olefin substrate. When gauging changes in the O−O bonding based on the metal populations of the different O−O derived levels of the peroxo complex, one has to take into account their nature as O−O bonding and *anti*-bonding, respectively. Molecular orbitals of **1A** with important contributions of the peroxide group are shown in Figure 7, right-hand column. It is convenient to classify these orbitals according to the dominant σ and π character with respect to their peroxo contribution. The role of the unoccupied σ* (O−O) level has already been discussed above; let us now consider the occupied O−O orbitals. Since the peroxo group coordinates side-on to the Ti center, each pair of O−O bonding π and *anti*-bonding π* orbitals splits. We shall designate the orbitals with a dominant contribution in the TiOO plane by $\pi_{||}$ or $\pi_{||}$* and those with a dominant contribution perpendicular to that plane by π* or π*. Based on energy considerations, donation from the *anti*-bonding $\pi_{||}$* and π* orbitals of the O_2^{2-} ligand to the vacant d-orbitals of the Ti d^0 center is expected to be strongest; in particular the $\pi_{||}$* orbital exhibits a strong overlap with the d_{yz} orbital of Ti (Figure 7). There is also considerable donation from the lower lying level $\pi_{||}$ (Figure 7). The contributions of the σ(O−O) and π* orbitals to the metal-peroxide interaction are less important for overlap reasons. This analysis is corroborated by an NBO calculation of the moiety TiO_2^{2+} in the geometry of **1A**. This model, which is free of hydroxide ligand contributions, allows a facile separation of the metal-π(O−O) interaction channels according to the various irreducible representations of the point group C_{2v}; however, metal populations may be too large since the ligand sphere is incomplete. The Ti d populations due to donation from $\pi_{||}$* and π* are 0.63 and 0.60 e, respectively; donation from the in-plane $\pi_{||}$* orbital is slightly larger for overlap reasons. Donation from the bonding O−O levels is smaller: 0.20 e from π* and 0.26 e compounded from $\pi_{||}$ and σ. The (stronger) donation from the $\pi_{||}$* and π* orbitals reduces the population of these O−O *anti*-bonding levels in the complex and thus leads to a strengthening of the peroxo bond, while donation from O−O bonding levels has a weakening effect.

This analysis helps to rationalize the changes in the structure of the peroxide group; in **1A**, the O−O bond is elongated by coordination to a Ti center, 1.487 Å (Table 1), compared to a gas phase H_2O_2 molecule (calc. 1.454 Å; exp. 1.452 Å[37]). Upon addition of base the O−O bond short-

ens to 1.47 Å in **1B** and 1.46 in **1C** while the activation barrier for oxygen transfer rises significantly, by 16 kcal/mol in **1C** compared to **1A** (Table 1, Figure 6c). These indicators are consistent with the interpretation that coordination of additional bases to the complex results in a stronger O−O bond with a concomitant increase in the electronic charge of the peroxide group. The question arises as to which of the peroxide orbitals discussed above gains more population as a consequence of the additional basic ligand: the O−O bonding or *anti*-bonding orbitals. Inspection of the orbital structure of **1B** (Figure 7, center column) helps to answer this question: donation to the d-orbital of Ti significantly stabilizes the lone pair of the NH_3 ligand in the complex (Figure 8): in **1B** the energy level that represents the lone pair of NH_3 appears in the same energy region as the bonding levels of the peroxide ligand and thus partially mixes with σ and $\pi_{||}$ levels (Figure 7). Mixing with the orbitals π and π* is essentially forbidden because these orbitals have a node in the TiOO plane where the NH_3 ligand approaches the complex. However, as can be seen from Figure 7, there is also almost no interaction between the NH_3 lone pair and the peroxide *anti*-bonding $\pi_{||}$* level. This may in part be rationalized by the much higher energy of the $\pi_{||}$* level, but also the nodal structure does not favor mixing with the NH_3 lone pair. One is therefore led to conclude that a basic ligand reduces donation from the O−O bonding $\pi_{||}$ orbital more strongly than from the O−O *anti*-bonding $\pi_{||}$* orbital.

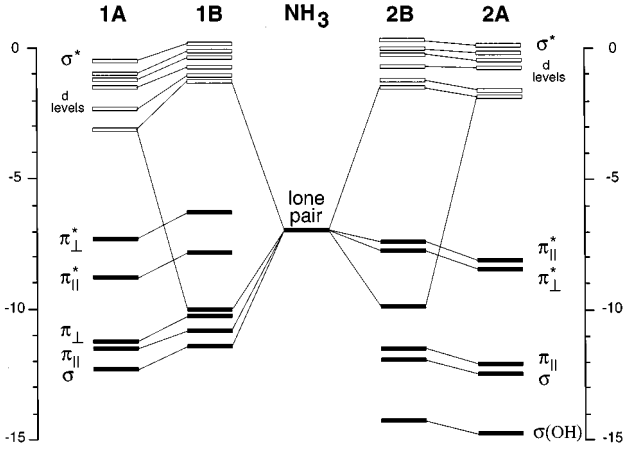

Figure 8. Orbital energy correlation diagram for peroxo and hydroperoxo derivatives

The above analysis shows that the bond between the metal center and the peroxo group plays an important role in the determination of the charge distribution over the orbitals of the peroxo moiety. This statement may be quantified with the help of an NBO charge analysis. The Ti contributions in the Ti−O σ interaction (in the TiOO plane) are 10% and 15% per bond for **1B** and **1C**, respectively. The corresponding contributions to the Ti−O π interaction (orthogonal to the TiOO plane) are 9% and 8% per bond for **1B** and **1C**, respectively. These small contributions of the metal center justify our idealized analysis focusing on the O−O derived orbitals. The increased Ti contributions in **1C** compared to **1B** indicate a strengthening of the Ti−O1 bond, in line with the calculated increase of the barrier for ethylene epoxidation. The elongation of the Ti−O1 bond from 1.84 Å in **1B** to 1.86 Å in **1C** (Table 1) may be due to stronger ligand-ligand repulsion in the highly coordinated **1C** species. However, the direct contribution of this bond to the activation energy should be considered as a second-order effect compared to the properties of the O−O bond. The main role of the Ti−O bond seems to be indirect: it influences the charge redistribution between the metal center and the peroxo group.

Figure 6 reveals that the hydroperoxo complexes follow similar general trends as the $Ti(O_2)$ complexes; however, they yield barriers of a similar height as complex **1A** despite their considerably shorter O−O bonds (Figure 6c). The orbital structure of the TiOOH species exhibits some peculiarities, which will be considered in the following discussion. When a proton is attached to the peroxo group, as in **2A** and **2B**, the electronic structure is significantly changed and a strong asymmetry is induced in the TiOO moiety (Figure 7, right-hand side). An idealized representation of the metal-ligand interaction in terms of OO orbitals has to be used with care for such species. The optimal position of the proton is in the plane almost orthogonal to the TiOO plane. Therefore, the strongest changes occur in the orbitals π and π*. The π contribution to O−O bonding is reduced and the nature of the resulting MO is better described as σ(OH) bonding; this level is the lowest in the orbital diagram of complex **2A** shown in Figure 7. In turn, the MO π* represents the lone pair of the center Oα of the hydroperoxo group (Figure 7). The other orbitals of the peroxo moiety (σ, $\pi_{||}$, and $\pi_{||}$*) remain more or less unchanged. The splitting of *anti*-bonding MOs π* and $\pi_{||}$*, with $\pi_{||}$* now being the HOMO, is significantly smaller, 0.3 eV for **2A**, than for $Ti(O_2)$ complexes where it amounts to more than 1 eV. The NBO analysis shows an almost equal charge distribution between the oxygen centers of the hydroperoxo group. The lower energy of the level 1s(Oβ) (Table 2) can be rationalized by the stabilization due to the electrostatic field of the attached proton.

As in the $Ti(O_2)$ complexes, addition of a donor ligand decreases the positive charge of the metal center, but its influence on the charge of the peroxo group is negligible (cf. the NBO charges and the core level energies of **2A** and **2B**; Table 2). At variance with the findings for "side-on" η^2-peroxo complexes, the additional ligand of the metal center has only a moderate effect on the activity of the hydroperoxo group. The calculated activation barrier of the intermediate **2B** even decreases slightly compared to **2A**. The negative charge of the peroxo group is higher in **2B** than in **2A** (Table 2) and, as a consequence, all pertinent valence levels are shifted upwards (Figure 8); however, this shift is smaller than that calculated when a ligand is introduced in **1A** to form **1B**. In particular, the vacant σ*(O−O) level shifts upwards by only 0.2 eV and its position is still rather low compared to $Ti(O_2)$ intermediates **1B** and **1C**,

which exhibit high barriers (Figure 6a). The apparently small effect of a basic ligand on the properties of the hydroperoxo complexes **2A/2B**, in particular on the oxygen transfer barrier, can be rationalized by the weaker metal-peroxo interaction in these "end-on" complexes. This follows, first of all, from the fact that only one oxygen atom, Oα, is involved in a strong interaction with the Ti center because the distance Ti−Oβ is much longer, by more than 0.3 Å (Table 2). Moreover, the Ti−Oα interaction is weaker than the corresponding interaction in the peroxo species. This can be inferred from the Ti−Oα distances in **2A** and **2B**, 1.89−1.92 Å, which are longer than the corresponding distances Ti−O of the peroxo complexes, 1.82−1.86 Å (Tables 1 and 2). Furthermore, the splitting of levels π* and $\pi_{||}$* is smaller in the hydroperoxo complexes due to reduced overlap with the orbitals of the metal center (Figure 7). The NBO analysis indicates a contribution of Ti to the Ti−Oα σ bond of 10% and 13% for **2A** and **2B**, respectively; this is slightly smaller than in the $Ti(O_2)$ complexes. However, at variance with the bonding of the $Ti(O_2)$ complexes, the π channel of the Ti−Oα interaction almost vanishes and the NBO analysis assigns the π* orbital to a lone pair located at the center Oα.

Coordination of the basic ligand NH_3 to **2A** and formation of species **2B** results in a slight decrease of the calculated activation barrier for the epoxidation of ethylene. This may be due to the fact that the lone pair of the NH_3 ligand of **2B** is stabilized in the gap between bonding and *anti*-bonding orbitals of the "peroxo" moiety. The bonding O−O levels of **2B** are lower in energy than the corresponding levels of the $Ti(O_2)$ intermediate **1B** while the NH_3 lone pair level is slightly higher (Figure 8). Inspection of the orbital structure of **2B** (Figure 7) shows that, in contrast to **1B**, this lone pair orbital of **2B** does not mix with the bonding O−O levels. In fact, this orbital even provides small contributions to the *anti*-bonding orbitals π*(OO) and $\pi_{||}$* (OO) that lie higher in energy. Thus, introduction of the additional basic ligand seems to affect the *anti*-bonding O−O levels of **2B** more than the bonding O−O levels. The resulting increased population of *anti*-bonding O−O levels leads to a weakening of the O−O bond and thus provides a rationalization for the small decrease in the barrier of the O−O bond activation in the epoxidation reaction.

Methyl Substitution of the Hydroperoxo Group

An important question is how a substituent R of the TiOOR moiety affects the epoxidation activity given that alkylhydroperoxides like *t*BuOOH are often used as oxidants.[1][3] To study this effect, we compare the epoxidation activity of the hydroperoxo complex **2A** with its methylperoxo derivative **3A** (Figure 2). Formation of **3A** according to the formal reaction **2A** + CH_3OH → **3A** + H_2O is exothermic by −4.9 kcal/mol. The calculated activation barrier for the complex **3A**, 15.8 kcal/mol, is 3 kcal/mol higher than that of **2A** (Table 2). The small increase of the negative charge on oxygen centers of the group $OOCH_3$ is in line with the weak electron-donating character of the methyl substituent; this inductive effect can also be detected from the small upward shift of 1s(O) levels (Table 2). Concomitantly, the σ*(O−O) level shifts upwards, correlating with an increase in the activation barrier (Figure 6a). The changes in the geometry of the peroxo moiety due to methyl substitution are minor.

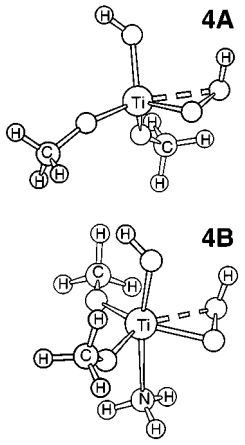

Figure 9. Model Ti hydroperoxo complexes, **4A** and **4B**, with equatorial hydroxide ligands replaced by methyloxide ligands

Methoxide and Siloxide in Comparison with Hydroxide Ligands

Finally, we consider the effects when hydroxide ligands of the model complexes are replaced by either methoxide or siloxide ligands. The methoxide derivatives **4A** and **4B** (Figure 9) are obtained from **2A** and **2B**, respectively, by formally exchanging two equatorial hydroxyl moieties by methoxide ligands. Analogous models with two $OSiH_3$ ligands will be referred to as **5A** and **5B**. These types of ligands are of interest since various titanium alkoxides, $Ti(OR)_4$, as well as titanium silicalites, are used as catalysts in epoxidation processes.[1]

In general, introduction of methoxide or siloxide ligands does not induce large structural changes in the TiOOH group (Table 2). The O−O bond length remains almost unchanged; the Ti−Oα distance becomes slightly shorter, while the Ti−Oβ distance increases somewhat. According to the NBO populations and the core level analysis, methoxide and siloxide ligands attract slightly more electron density from the Ti center than the hydroxide ligands. Thus, the electron density on the peroxo oxygen centers of the complexes **4A** and **4B** is higher (by 0.02 and 0.01 e) than on those of **2A** and **2B**, respectively; concomitantly, the 1s(O) levels shift to less negative energies by 0.2−0.3 eV. On the other hand, in complexes **5A** and **5B** there is somewhat less electron density on the peroxo group (compared to **2A** and **2B**, respectively), although for **5B** it can be detected only from the negative shift, −0.2 eV, of 1s(O) levels. Both types of ligands lead to slightly increased barriers of ethylene epoxidation. As in **2B**, the additional basic ligand NH_3 in **4B** and **5B** reduces the activation barriers by 0.9 and 1.3

kcal/mol compared to **4A** and **5A**, respectively. The corresponding transition states do not exhibit any noteworthy structural differences. Addition of NH_3 to **4A** and **5A** is exothermic by −11.0 and −12.1 kcal/mol, respectively. Based on the experience with the TiOOH models we expect similarly minor changes in the properties of the TiOO moieties due to substitution of hydroxide ligands by methoxide or siloxide.

A recent computational study of Ti silicalites[24] by Sinclair and Catlow also included a DF-BP86 calculation of ethylene epoxidation by the complex $(H_3SiO)_2Ti(OH)OOH$, which is essentially the same as the present model **5A**. For that model an activation barrier of 10.3 kcal/mol was calculated,[24] which is lower than the present result of the hybrid B3LYP, but is in agreement with the trend[34][35] of "pure" DF functionals like BLYP and BP86 in yielding lower barriers than the B3LYP hybrid method, which partially accounts for exact exchange. Sinclair and Catlow also considered the transformation of the structure $(H_3SiO)_2Ti(OH)OOH$ to $(H_3SiO)_2Ti(OH_2)(O_2)$ by an internal proton transfer, which is analogous to the transformation of **1B′** to **2A**.[24] In that study, contrary to the present results for **1B′** and **2A**, the $Ti(O_2)$ species was found to be more stable than the TiOOH analogue by about −10 kcal/mol. This difference may be due either to the different exchange-correlation potentials used or the influence of the $OSiH_3$ ligands. Sinclair and Catlow considered the structure $(H_3SiO)_2Ti(OH_2)(O_2)$ as a poisoned form of the catalyst, but they did not prove its inertness in the epoxidation process by calculating the corresponding transition state.[24] Under reaction conditions, a further base will coordinate to the Ti center; comparison with our models **1B** and **1B′** shows that adding one more basic ligand to $(H_3SiO)_2Ti(OH_2)(O_2)$ will render the activation barrier even higher.

Conclusions

We have studied the epoxidation of ethylene by model Ti^{IV} peroxo complexes with both "side-on" peroxo $Ti(\eta^2-O_2)$ and "end-on" hydroperoxo (or alkylperoxo) TiOOR (R = H, CH_3) moieties by means of hybrid B3LYP density functional calculations. The low coordinated intermediate $(HO)_2Ti(O_2)$ was found to exhibit a relatively low barrier of oxygen transfer, however it is not thermodynamically stable since it readily forms base adducts (Figure 5). Coordination of additional donor ligands to the Ti center (**1B**, **1C**) significantly increases the activation energy of a $Ti(O_2)$ group. Participation of the most stable intermediate **1C**, with its saturated coordination sphere, in the epoxidation process is ruled out for kinetic reasons since the corresponding transition state exhibits a high barrier, above 27 kcal/mol. The inhibiting effect of donor ligands was rationalized with the help of a molecular orbital analysis. Two effects were distinguished: (i) additional basic ligands reduce the electrophilicity of the peroxo group and push the σ*(O−O) orbital responsible for breaking the O−O bond to higher energies; (ii) concomitantly, the populations of the bonding levels of the peroxo group increase and strengthen the O−O bond, as deduced from shorter O−O distances in model complexes with higher coordination numbers. The high activation barrier for coordinatively saturated $Ti(O_2)$ species is in agreement with the experimentally observed chemical stability of known Ti^{IV} peroxo complexes.[10][11]

At variance with $Ti(O_2)$ moieties, the activity of a TiOOH functional group depends only very weakly on the saturation of the Ti coordination sphere. The hydroperoxo group is less sensitive to the coordination of the Ti center since there are less channels for metal-peroxo interaction for such "end-on" structures than in the case of symmetric "side-on" structures $Ti(O_2)$. Calculated reaction energies and activation barriers show that Ti hydroperoxo species are very favorable for thermodynamic *and* kinetic reasons. The hydroperoxo complex **2B**, with one basic ligand, is only slightly less stable than the η^2-peroxo complex **1C** with two basic ligands. Due to its low activation barrier, it exhibits by far the lowest lying transition state (by absolute energy, Figure 5). Substitution of hydrogen by methyl in the TiOOR group (**2A** vs. **3A**) was found to increase the activation barrier for epoxidation by 3 kcal/mol. Substitution of hydroxide anionic ligands in TiOOH model complexes by alkyloxide and siloxide increases the activation barrier by 1−2 kcal/mol. The activation barriers of oxygen transfer from a TiOOR group to an ethylene molecule are calculated in the range of 13−16 kcal/mol, thus are comparable, if not lower, than the barriers calculated at the same level of computation for various Re peroxo species.[17]

In summary, the computational results favor reaction paths that involve hydroperoxo (or alkylperoxo) titanium species over $Ti(O_2)$ species. Thus, the results of the present computational study support the interpretation of experimental and theoretical studies[4,7,10,15] that hydroperoxo intermediates are responsible for the epoxidation reactions by Ti complexes and Ti-silicalites, while the corresponding peroxo species appear (if at all) as a chemically inert structures of side reactions only.

Computational Details

In the density functional calculations[38] we employed the hybrid B3LYP exchange-correlation scheme.[39] The 1s, 2s, and 2p core shells of Ti were replaced by a LANL2 effective core potential (ECP).[40] The corresponding basis set[40] of Ti, which describes the outermost core (3s and 3p) and the valence shells, was used in the contraction (441/2111/41). For main group elements we employed a 6-311G(d,p) basis set.[33] Geometry optimizations of intermediates and transition states were performed without any symmetry constraints. Transition state structures were searched by numerically estimating the matrix of second-order energy derivatives at every optimization step and by requiring exactly one eigenvalue of this matrix to be negative. We checked typical transition state structures by performing a full vibrational analysis, using a TZV basis set for Ti (see below). Reaction energies and barrier heights were evaluated in single-point fashion with the Ti basis set augmented by a polarization f-exponent (1.506).[42]

To check how results depend on the quality of basis set and to validate the ECP for the present study, some model complexes and the corresponding transition states (including a full vibrational analysis) were re-calculated using an all-electron valence triple-ζ (TZV) basis set for Ti (842111/6311/411). Reaction energies and barrier heights were evaluated in single-point calculations with an augmented Ti basis, using the above polarization f-exponent [TZV(f)].

In preceding studies of Re and Mo oxo and peroxo complexes[17][29] zero-point energy corrections were shown to uniformly shift the calculated reaction energies and reaction barriers by small positive values. However, in no case did they change the qualitative picture when reactivity of different intermediates was compared. Therefore, in the present study we refrained from applying zero-point energy corrections to reaction energies and barrier heights.

Acknowledgments

We thank P. Hofmann, H. Rothfuss, J. H. Teles, and G. N. Vayssilov for helpful discussions. This work was supported by the Deutsche Forschungsgemeinschaft, the German Bundesministerium für Bildung, Wissenschaft, Forschung und Technologie (grant no. 03D0050B), INTAS-RFBR (IR-97−1071), and the Fonds der Chemischen Industrie.

[1] K. A. Jørgensen, *Chem. Rev.* **1989**, *89*, 431−458.
[2] T. Katsuki, K. B. Sharpless, *J. Am. Chem. Soc.* **1980**, *102*, 5974−5976.
[3] R. A. Sheldon, *J. Mol. Catal.* **1980**, *7*, 107−126.
[4] M. G. Clerici, P. Ingallina, *J. Catal.* **1993**, *140*, 71−83.
[5] G. Tozzola, M. A. Mantegazza, G. Ranghino, G. Petrini, S. Bordiga, G. Ricchiardi, C. Lamberti, R. Zulian, A. Zecchina, *J. Catal.* **1998**, *179*, 64−71.
[6] G. N. Vayssilov, *Catal. Rev. Sci. Eng.* **1997**, *39*, 209−251.
[7] M. G. Finn, K. B. Sharpless, *J. Am. Chem. Soc.* **1991**, *113*, 113−126.
[8] B. Notari, *Stud. Surf. Sci. Catal.* **1988**, *37*, 413−425.
[9] D. R. C. Huybrechts, L. De Bruycker, P. A. Jacobs, *Nature* **1990**, *345*, 240−242.
[10] H. J. Ledon, F. Varescon, *Inorg. Chem.* **1984**, *23*, 2735−2737.
[11] H. Mimoun, M. Postel, F. Casabianca, J. Fischer, A. Mitschler, *Inorg. Chem.* **1982**, *21*, 1303−1306.
[12] H. Mimoun, in: *Chemistry of Peroxides*, (Ed.: S. Patai), Wiley, Chichester, **1983**, Chapter 15, pp. 463−482.
[13] C. C. Romão, F. E. Kühn, W. A. Herrmann, *Chem. Rev.* **1997**, *97*, 3197−3246.
[14] H. Mimoun, I. S. de Roch, L. Sajus, *Tetrahedron* **1970**, *26*, 37−50.
[15] G. Amato, A. Arcoria, F. P. Ballistreri, G. A. Tomasseli, O. Bortolini, V. Conte, F. Di Furia, G. Modena, G. Valle, *J. Mol. Catal.* **1986**, *37*, 165−175.
[16] E. P. Talsi, K. V. Shalyaev, K. I. Zamaraev, *J. Mol. Catal.* **1993**, *83*, 347−366.
[17] P. Gisdakis, S. Antonczak, S. Köstlmeier, W. A. Herrmann, N. Rösch, *Angew. Chem.* **1998**, *110*, 2333−2336; *Angew. Chem. Int. Ed.* **1998**, *37*, 2211−2214.
[18] F. E. Kühn, A. M. Santos, P. W. Roesky, E. Herdtweck, W. Scherer, P. Gisdakis, I. V. Yudanov, C. Di Valentin, N. Rösch, *Chem. Eur. J.* **1999**, in press.
[19] C. Di Valentin, P. Gisdakis, I. V. Yudanov, N. Rösch, in preparation.
[20] Y. D. Wu, D. K. W. Lai, *J. Org. Chem.* **1995**, *60*, 673−680.
[21] E. Karlsen, K. Schöffel, *Catal. Today* **1996**, *32*, 107−114.
[22] [22a] G. M. Zhidomirov, A. L. Yakovlev, M. A. Milov, N. A. Kachurovskaya, I. V. Yudanov, *Catal. Today* **1999**, *51*, 1−14. − [22b] I. V. Yudanov, Ph. D. Dissertation, Boreskov Institute of Catalysis, Novosibirsk, **1997**.
[23] D. Tantanak, M. A. Vincent, I. H. Hillier, *Chem. Commun.* **1998**, 1031−1032.
[24] P. E. Sinclair, C. R. A. Catlow, *J. Phys. Chem.* **1999**, *103*, 1084−1095.
[25] H. Manohar, D. Schwarzenbach, *Helv. Chim. Acta* **1974**, *57*, 1086−1095.
[26] R. Guilard, J.-M. Latour, C. Lecomte, J.-C. Marchon, J. Protas, D. Ripoll, *Inorg. Chem.* **1978**, *17*, 1228−1237.
[27] G. Boche, K. Möbus, K. K. Harms, M. Marsch, *J. Am. Chem. Soc.* **1996**, *118*, 2770−2771.
[28] A. Zecchina, S. Bordiga, C. Lamberti, G. Ricchiardi, D. Scarano, G. Petrini, G. Leofanti, M. Mantegazza, *Catal. Today* **1996**, *32*, 97−106.
[29] P. Gisdakis, S. Antonczak, N. Rösch, *Organometallics*, in press.
[30] D. A. Singleton, S. R. Merrigan, J. Liu, K. N. Houk, *J. Am. Chem. Soc.* **1997**, *119*, 3385−3386.
[31] R. D. Bach, C. M. Estévez, J. E. Winter, M. N. Glukhovtsev, *J. Am. Chem. Soc.* **1998**, *120*, 680−685.
[32] W. Adam, D. Golsch, J. Sundermeyer, G. Wahl, *Chem. Ber.* **1996**, *129*, 1177−1182.
[33] W. R. Thiel, T. Priermeier, *Angew. Chem.* **1995**, *107*, 1870−1871; *Angew. Chem. Int. Ed. Engl.* **1995**, *34*, 1737−1738.
[34] J. Baker, M. Muir, J. Andzelm, *J. Chem. Phys.* **1995**, *102*, 2063−2079.
[35] A. Görling, S. B. Trickey, P. Gisdakis, N. Rösch, in: *Topics in Organometallic Chemistry*, Vol. 4, (Eds.: J. Brown, P. Hofmann), Springer, Berlin, **1999**, p. 109.
[36] A. E. Reed, L. A. Curtiss, F. Weinhold, *Chem. Rev.* **1988**, *88*, 899−926.
[37] *CRC Handbook of Chemistry and Physics*, 73rd Ed., CRC Press, Boca Raton, FL, **1993**.
[38] *Gaussian 94*, Revision D.4, M. J. Frisch, G. W. Trucks, H. B. Schlegel, P. M. W. Gill, B. G. Johnson, M. A. Robb, J. R. Cheeseman, T. Keith, G. A. Petersson, J. A. Montgomery, K. Raghavachari, M. A. Al-Laham, V. G. Zakrzewski, J. V. Ortiz, J. B. Foresman, J. Cioslowski, B. B. Stefanov, A. Nanayakkara, M. Challacombe, C. Y. Peng, P. Y. Ayala, W. Chen, M. W. Wong, J. L. Andres, E. S. Replogle, R. Gomperts, R. L. Martin, D. J. Fox, J. S. Binkley, D. J. Defrees, J. Baker, J. P. Stewart, M. Head-Gordon, C. Gonzalez, J. A. Pople, Gaussian, Inc., Pittsburgh PA, **1995**.
[39] [39a] A. D. Becke, *J. Chem. Phys.* **1993**, *98*, 5648−5651. − [39b] C. Lee, W. Yang, R. G. Parr, *Phys. Rev. B* **1988**, *37*, 785−789.
[40] P. J. Hay, W. R. Wadt, *J. Chem. Phys.* **1985**, *82*, 299−310.
[41] R. Krishnan, J. Binkley, R. Seeger, J. Pople, *J. Chem. Phys.* **1980**, *72*, 650−654.
[42] A. W. Ehlers, M. Böhme, S. Dapprich, A. Gobbi, A. Höllwarth, V. Jonas, K. F. Köhler, R. Stegmann, A. Veldkamp, G. Frenking, *Chem. Phys. Lett.* **1993**, *208*, 111−114.
[43] A. Schäfer, C. Huber, R. Ahlrichs, *J. Chem. Phys.* **1994**, *100*, 5829−5835.

Received June 18, 1999
[I99226]